Kornberg, A. (1980) in *DNA Replication*, W. H. Freeman, San Francisco, CA.
Kornberg, A. (1982) in *Supplement to DNA Replication*, W. H. Freeman, San Francisco, CA.
Lawton, K. G., Wierowski, J. V., Schechter, S., Hilf, R., & Bambara, R. A. (1984) *Biochemistry 23*, 4294–4300.
Maniatis, T., Fritsch, E. F., & Sambrook, J. (1982) in *Molecular Cloning: A Laboratory Manual*, Cold Spring Harbor Laboratory, Cold Spring Harbor, NY.
Masaki, S., Koiwai, O., & Yoshida, S. (1982) *J. Biol. Chem. 257*, 7172–7177.
McClure, W. R., & Jovin, T. M. (1975) *J. Biol. Chem. 253*, 413–423.
McClure, W. R. & Chow, Y. (1982) *Methods Enzymol. 64*, 277–295.
McKune, K., & Holmes, A. M. (1979) *Biochem. Biophys. Res. Commun. 90*, 864–870.
Nakayama, K., & Sugino, A. (1980) *Biochem. Biophys. Res. Commun. 96*, 306–312.
Oguro, M., Suzuki-Hori, C., Naguno, H., Mano, Y., & Ikegami, S. (1979) *Eur. J. Biochem. 97*, 603–607.
Riedel, H.-D., König, H., & Knippers, R. (1984) *Biochim. Biophys. Acta 783*, 158–165.
Rusquet, R., Bohommet, M., & David, J. C. (1984) *Biochem. Biophys. Res. Commun. 121*, 762–769.
Schomburg, U., & Grosse, F. (1986) *Eur. J. Biochem. 160*, 451–457.
Tabor, C. W., & Tabor, H. (1984) *Annu. Rev. Biochem. 53*, 749–790.
Villani, G., Fay, P. J., Bambara, R. A., & Lehman, I. R. (1981) *J. Biol. Chem. 256*, 8202–8207.
Wahl, A. F., Kowalski, S. P., Harwell, L. W., Lord, E. M., & Bambara, R. A. (1984) *Biochemistry 23*, 1895–1899.
Wang, T. S.-F., Hu, S.-Z., & Korn, D. (1984) *J. Biol. Chem. 259*, 1854–1865.
Wierowski, J. V., Lawton, K. G., Hockensmith, J. W., & Bambara, R. A. (1983) *J. Biol. Chem. 258*, 6250–6254.
Wilson, S. H., Matsukage, A., Bohn, E. W., & Sivarajan, M. (1977) *Nucleic Acids Res. 4*, 3981–3996.
Yamamoto, K. R., Alberts, B. M., Benzinger, R., Lawhorn, L., & Treiba, G. (1970) *Virology 40*, 734–744.

Protein-Dependent Conformational Behavior of DNA in Chromatin†

Martin R. Riehm and Rodney E. Harrington*
Department of Biochemistry, University of Nevada, Reno, Reno, Nevada 89557
Received August 28, 1986; Revised Manuscript Received December 4, 1986

ABSTRACT: Information from circular dichroism (CD) and DNA thermal denaturation has been used in concert to study the conformational behavior of DNA in the extended 11-nm fiber of chromatin isolated from HeLa nuclei. The histone-dependent conformational states of the system were investigated by selectively removing the hydrophilic histone domains with trypsin. These were compared to acetylated chromatin from the same source. The integrated intensity of the positive CD band for DNA above 260 nm is found to increase with the content of relatively unstressed B-form DNA. This same increase is observed along the series of whole, H1-stripped, and trypsinized chromatin samples as protein is removed. Hence, the ratio of percent hyperchromicity to integrated CD band intensity of the respective melting transitions provides useful information on the conformational state of DNA in the three principal regions of the chromatin fiber: the central loop and flanking nucleosomal regions and the linker. Results from this study suggest that central loop DNA in both hyperacetylated and control chromatin relaxes as protein is removed. However, hyperacetylated chromatin shows significantly less dependence than control chromatin upon core histone hydrophilic domains in the flanking and linker regions. Thus, histone hyperacetylation evidently relaxes DNA in chromatin with no major overall conformational changes. A possible role of histone hyperacetylation may therefore be to reduce cooperativity in the unfolding transition in chromatin and thus provide for greater localized control of unfolding during transcription.

Trypsin proteolysis has been used to probe the structural function of the N-terminal and C-terminal histone protein domains in chromatin [reviewed in Bohm and Crane-Robinson (1984)]. Trypsin digests of chromatin yield a stable series of peptides at maximal proteolysis which have been identified as core histone C-terminal regions with the N-terminal regions preferentially cleaved (Crane-Robinson & Bohm, 1985). At this level of proteolysis, some C-terminal residues of histone H2A (and at times H3) are also cleaved.

Earlier trypsin digestion studies have shown that the highly conserved C-terminal core histone domains are capable of folding DNA into compact nucleosome-like particles (Whitlock & Stein, 1978). These trypsinized core particles appear to unfold from the DNA ends on either side of the 80 base pair central core loop (Lilley & Tatchell, 1977). The unfolding process seems to be reversible, and the transition occurs at about 0.1 M sodium ion concentration (Grigoryev & Krasheninnikov, 1982). Other studies with chromatin fragments have shown that the hydrophilic domains of the core histones are necessary to condense chromatin into the 30-nm solenoid (Allan et al., 1982; Marion et al., 1983). The N-terminal domains of core histones, which also contain the in vivo acetylation sites, therefore appear to play a structural role in

† This work was supported by U.S. Public Health Service Grant GM 33435 and by Hatch Project 131 from the College of Agriculture, University of Nevada, Reno.
* Address correspondence to this author.

0006-2960/87/0426-2878$01.50/0

tightly folding DNA into nucleosomes and further condensing chromatin into higher order fibers.

The results reported here suggest that the flanking DNA of nucleosomes in the 11-nm fiber of chromatin is a center of structural lability. This is in accord with a number of earlier observations. Simpson (1978) showed that histone hyperacetylation increases nuclease sensitivity in flanking DNA. Studies on the conformational transition in low-salt media suggest also that flanking DNA unfolds from the core, leaving approximately one superhelical loop of DNA at ionic strengths below 3 mM sodium (Uberbacher et al., 1983; Harrington, 1981, 1982; Wu et al., 1979). A similar type of unraveling may also occur at high salts above 450 mM sodium (Harrington, 1982; Russev et al., 1980; Wilhelm & Wilhelm, 1980). Trypsinization of the hydrophilic histone domains has been functionally equated to acetylation in its effects on chromatin structure (Allan et al., 1982). Grigoryev and Krasheninnikov (1982) and Lilley and Tatchell (1977) have reported dramatic effects on nucleosome structure and stability due to core histone trypsinization which they associate with flanking DNA. Thus, we believe that core histone tails are capable of stabilizing intranucleosomal DNA as proposed by Yau et al. (1982) and that this function evidently occurs but is not restricted to the flanking region.

Acetylation is one of several postsynthetic histone modifications associated with DNA replication and transcription [reviewed in Matthews and Waterborg (1985)], spermatogenesis (Christensen et al., 1984), and DNA repair (Smith, 1986). It occurs primarily in the N-terminal regions of core histones. Sodium butyrate has been widely used in recent studies to promote the accumulation of hyperacetylated histone by inhibiting histone deacetylase (Sealy & Chalkley, 1978). At maximum acetylation, up to 17% of the total positive charge on the histone octamer is neutralized, with over 60% neutralized on the histone N-terminal domains. Despite the potential loss of histone–DNA interaction, butyrate-induced acetylation has little effect upon the conformation of DNA in nucleosome core particles (Ausio & Van Holde, 1986) or the condensation of chromatin into the 30-nm fiber (Dimitrov et al., 1986; McGhee et al., 1983).

Presently, data concerning the stability of acetylated chromatin are inconclusive. Huvos et al. (1984), using circular dichroism (CD)[1] and DNA thermal denaturation (TD), observe no differences in the stability of chromatin isolated from butyrate-treated cells and reconstituted with histone H1 from rat thymus. Sasi and Fasman (1984) also report identical melting behavior for control and hyperacetylated H1-stripped chromatin. On the other hand, Yau et al. (1983), also using TD, demonstrate significant decreases in the stability of acetylated nucleosome core oligomers in the absence of histone H1, specifically within the nuclease-resistant central loop DNA. The association of melting transitions with specific structural regions of chromatin is also a complex problem which has not yet been fully resolved (Yau et al., 1983; Reczek et al., 1982; Weischet et al., 1978). Finally, special difficulties arise when the sodium butyrate method is used due to evident increases in histone H1 content, especially the variant H1° (Hall & Cole, 1985). All these uncertainties suggest that further studies are required on the roles of core histone tails and their acetylation levels in chromatin structure–function relationships.

We have used circular dichroism and high-resolution thermal denaturation to study the conformational behavior of DNA in three principal regions of differing stability in the 11-nm fiber of chromatin. Results from both techniques depend strongly upon the integrity of the core histones (Lilley & Tatchell, 1977; Hjelm & Huang, 1974). Our approach differs from earlier studies in that we correlate the chiral behavior of the DNA with informaiton on conformational stability available from thermal denaturation. H1-stripped chromatin was exposed to increasing concentrations of trypsin to remove selectively and differentially the nonstructured histone tails. CD and TD data were obtained on these preparations at 5 and 0.2 mM sodium ion concentration. Using the correlation between percent hyperchromicity and integrated molar ellipticity for the three resolved thermal denaturation transitions, we can assign these transitions to three regions of differential stability in the chromatin DNA and deduce the relative conformational behavior of these regions in control vs. hyperacetylated chromatin.

Materials and Methods

The chromatin used in all experiments reported was obtained from HeLa cell nuclei. Cells were grown in suspension culture with or without 7 mM sodium butyrate treatment according to the method of Yau et al. (1982). Both control chromatin and hyperacetylated chromatin was solubilized with mild micrococcal nuclease (Worthington) digestion and low ionic strength extraction according to the methods of Reczek et al. (1982) with RNase A (Worthington) treatment according to McGhee et al. (1983). A polynucleosomal fraction of from $n = 2$ to about 30 was obtained by using Bio-Gel A-15M chromatography according to the method of Reczek et al. (1982).

To determine the role of protein–DNA interactions in nucleosome stability, we selectively degraded the histone components of chromatin. Whole chromatin samples were stripped of H1 histone by using carboxymethyl ion-exchange chromatography at 50 mM sodium chloride/10 mM Tris at pH 7.8 as described by Libertini and Small (1980). H1-stripped chromatin samples were trypsinized in the same buffer using trypsin enzyme activities comparable to those previously reported (Weintraub & Van Lente, 1974; Allan et al., 1982; Figure 1). Proteolytic digestion was allowed to proceed for 1–4 h at 0 °C and was stopped by adding soybean trypsin inhibitor (Sigma, type II-S) according to the method of Allan et al. (1982).

All preparative buffers contained 5 mM sodium butyrate to prevent loss of acetylation in the histones as discussed by Yau et al. (1982). All experimental runs were completed within 3 weeks of preparation.

HeLa DNA was prepared by using standard methods of proteinase K digestion of whole and trypsinized samples, extracted 3 times with phenol/chloroform followed by precipitation by addition of 2–3 volumes of 90/96/100% ethanol. To reduce residual phenol content, the DNA was reprecipitated 3 times from 70% ethanol. HeLa DNA isolated from all chromatin preparations was protein free as judged by the Lowry method.

Sample Characterization. Potential nucleosome sliding was monitored by using the methods of Noll et at. (1975). Whole and H1-stripped chromatin samples were redigested with various micrococcal nuclease concentrations at 4 °C for 30 min. Extracted DNA was run on 1.7% agarose gels in

[1] Abbreviations: CD, circular dichroism; TD, DNA thermal denaturation; T_m, temperature of maximum dh/dT for each transition; Tris, tris(hydroxymethyl)aminomethane; PMSF, phenylmethanesulfonyl fluoride; SDS, sodium dodecyl sulfate; EDTA, ethylenediaminetetraacetic acid; R_x/R_0, integrated molar ellipticity of the sample normalized by the integrated molar ellipticity of purified DNA for the CD band above 260 nm; G-C, guanine–cytosine nucleotide bases; bp, base pair(s).

Tris/borate/EDTA buffer. Photographs of the ethidium bromide stained gels were scanned at high resolution (Waterborg & Harrington, 1986; Waterborg et al., 1987), and fragment sizes were determined in relation to ϕX174/*Hae*III restriction fragment markers.

Protein concentration was determined by the procedure of Lowry et al. (1951), using the bovine serum albumin to histone conversion factor of Reczek et al. (1982). DNA content was determined by the optical density at 258 nm where an A_{1cm} of 20 = 1 mg of DNA. Acid–urea–polyacrylamide slab gels were run according to the method of Hardison and Chalkley (1978) with modifications for sample treatment as given by Reczek et al. (1982). Histone SDS–polyacrylamide gel electrophoresis was done according to the method of Laemmli (1970) as modified by Thomas and Kornberg (1975). Photographic negatives of Coomassie blue stained gels were scanned at high resolution as discussed above.

Thermal Denaturation. Thermal melting of whole chromatin samples was done on a Gilford Model 252 UV–visible spectrophotometer equipped with a Model 2527 thermoprogrammer. All samples were dialyzed to 0.2 mM EDTA at pH 7.0 and used directly, or stock NaH_2PO_4 was added to 5 mM. All samples, at OD_{260} = 0.75, were degassed under vacuum at or below room temperature before use.

Temperature was calibrated and monitored from within the housing of the cuvette holder. The temperature increase was maintained at 0.25 °C/min. The chart recording of the temperature-dependent hyperchromicity monitored at 260 nm was digitized at 0.23 °C increments into a Hewlett-Packard 85B microcomputer equipped with a Model 7225A plotter. Base-line corrections were made by running a buffer blank for each thermal denaturation run and subtracting it from each melting curve in the run.

Derivative melting curves were obtained by taking a floating linear least-squares slope at each point of the digitized thermal melting data. We found this method somewhat faster and equally satisfactory to higher order polynomial fits or cubic spline derivatives followed by repetitive Chebychev polynomial filtering. Melting curves were resolved into three overlapping Gaussians by using the least-squares band-fitting program of Fraser and Suzuki (1966) as revised by Burkhart and Howells (1979). This program uses an algorithm in which estimates for peak amplitude, half-width, and center are input and are refined by iterative solution of a set of linear simultaneous equations with the constraint that the standard error between the observed and calculated curve points is minimized. Divergence is avoided by using a damping procedure.

Circular Dichroism. Parallel measurements of absolute CD spectra between 250 and 320 nm for each sample were obtained by using a Jasco Model J-40A spectropolarimeter equipped with a Model DP-501 data processor and calibrated with 10-camphorsulfonic acid. The spectra were obtained at 5 mM sodium phosphate/0.2 mM EDTA. The spectral points, obtained as ΔA, were digitized at 0.5-nm increments and derived in terms of molar nucleotide residue ellipticity using an extinction coefficient at 258 nm of 6800 cm^{-1} (mol of nucleotide)$^{-1}$. The integral of the positive spectral band above 260 nm was obtained by computer using Simpson's rule.

Results

Sample Characteristics. Control and hyperacetylated whole chromatin samples had similar average protein/DNA ratios of 1.37 ± 0.09 and 1.39 ± 0.06, respectively, after treatment with RNase A to remove endogenous ribonucleoprotein. Published protein/DNA ratios using comparable isolation techniques are 1.3 without RNase treatment (Reczek et al., 1982). For both types of chromatin, RNase treatment resulted in a loss of optical density at 258 nm of about 30% as reported previously (McGhee et al., 1983). H1-stripped chromatin had average protein/DNA ratios of 1.13 ± 0.05 for control samples and 1.08 ± 0.04 for hyperacetylated samples. Both types of samples show the normal complement of five histones on SDS–polyacrylamide gels (Figure 1). Lanes 2 and 7 of Figure 1 show that chromatin samples suffer a small amount of proteolysis during isolation.

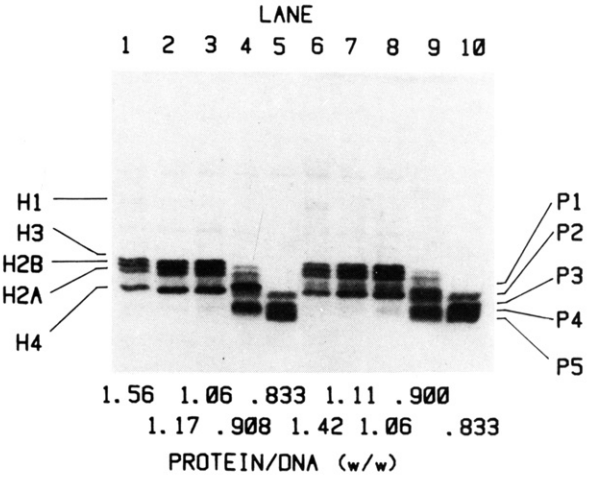

FIGURE 1: SDS–PAGE of control (lanes 1–5) and hyperacetylated (lanes 6–10) trypsinized chromatin. Bovine pancreas trypsin EC 3.4.21.4) type III from Sigma was used to degrade H1-stripped preparations of control (lane 2) and hyperacetylated (lane 7) chromatin. The trypsin concentrations used were 0.625 pg/mL (lanes 3 and 8), 62.5 pg/mL (lanes 4 and 9), and 625 pg/mL (lanes 5 and 10). Sample concentrations were 1–2 A_{260} units for trypsinizations.

These gels also show that the amino-terminal regions of the four core histones in stripped, trypsinized fractions were selectively and differentially removed as reported previously (Weintraub & Van Lente, 1974) with some variation under the conditions reported here. The remaining lanes of Figure 1 reveal a pattern of trypsin activity-dependent digestion in which H3 and H4 histones are attacked first. Histone H4 seems to persist at slightly higher trypsin activities for both control and hyperacetylated chromatin. Histones H2A and H2B begin to degrade after H3 is completely digested. In our hands, maximum trypsinization yielded a loss of about 24% in core histone protein content, with protein/DNA ratios of 0.83. This ratio is comparable to results of 0.7–0.8 given by Whitlock and Simpson (1977) for maximally trypsinized HeLa chromatin.

The butyrate-treated chromatin samples were highly acetylated as shown on acid–urea gels (data not shown) and as previously demonstrated (Riggs et al., 1977). Hyperacetylated chromatin was used as extracted. Quantitation of the five acetylated species of histone H4 in our acid–urea gels gave an average of 0.31 acetyl group per H4 for control chromatin and 2.1 acetyl groups per H4 for hyperacetylated chromatin. High-resolution densitometric scans of the various lanes in Figure 1 and other SDS gels (data not shown) showed some variation in trypsin cleavage products of hyperacetylated histones. These can be interpreted by using cleavage products identified by Bohm and Crane-Robinson (1984) and shown in Figure 1. Overall, histone acetylation had no major effect on trypsinolysis of the four core histones and resulted in only minor variations in the cleavage products. At maximum trypsinization, hyperacetylated samples showed relative increases in the cleavage product P4 over P5, both from histone H4. Also, the unresolved band containing cleavage products P1, P2, and P3 is much broader for hyperacetylated histones,

Table I: Summary of Results for Chromatin Thermal Melting Studies

sample	transition	T_m[a]	mean width[b]	% H_t[c]	DNA (bp)[d]
		5.25 mM Sodium Ion Concentration			
control					
whole	I	67.8 ± 0.9	4.68	9.6 ± 1.1	20
	II	73.2 ± 0.9	4.35	18.0 ± 5.0	36
	III	81.8 ± 0.3	4.98	72.3 ± 4.9	147
H1 stripped	I	63.4 ± 1.2	6.09	17.8 ± 3.4	36
	II	72.7 ± 1.4	7.72	33.2 ± 7.0	67
	III	81.7 ± 1.3	4.94	49.0 ± 4.5	99
hyperacetylated					
whole	I	68.1 ± 0.3	5.56	10.3 ± 3.2	21
	II	72.6 ± 0.4	4.43	19.2 ± 3.1	39
	III	80.8 ± 0.8	4.80	70.6 ± 4.1	143
H1 stripped	I	63.5 ± 1.1	7.17	37.1 ± 3.8	75
	II	72.9 ± 1.1	5.02	15.3 ± 2.4	31
	III	81.2 ± 0.9	5.20	47.6 ± 3.6	96
		0.20 mM Sodium Ion Concentration			
control					
whole	I	61.2 ± 1.9	7.05	8.9 ± 3.1	18
	II	72.8 ± 1.5	7.76	36.4 ± 3.4	74
	III	79.4 ± 0.3	4.90	54.7 ± 0.6	111
H1 stripped	I	50.5 ± 0.1	8.75	29.3 ± 2.6	59
	II	70.3 ± 4.0	9.81	37.1 ± 11.8	75
	III	80.3 ± 1.6	5.08	33.5 ± 12.7	68
hyperacetylated					
whole	I	61.6 ± 1.9	6.60	11.4 ± 2.1	23
	II	70.6 ± 1.7	6.28	26.8 ± 2.1	54
	III	78.4 ± 0.7	5.54	61.9 ± 4.1	126
H1 stripped	I	48.3 ± 1.6	8.45	32.1 ± 2.6	65
	II	69.3 ± 2.1	10.3	39.4 ± 11.0	80
	III	79.3 ± 0.4	4.83	28.5 ± 9.0	58

[a] The transition melting point in degrees centigrade [b] The width of the transition in degrees at $1/e$ maximum height. [c] The percent total observed hyperchromicity. [d] The amount of DNA melting in the transition based on a nucleosomal repeat of 203 bp.

indicating greater diversity in the series of cleavage products from histones H3, H2A, and H2B. This agrees with sequencing studies on limit digests which show that of the four core histones, only H2B has a tryptic cutting site at a lysine residue which is acetylated in vivo (Bohm & Crane-Robinson, 1984).

Both control and butyrate-treated whole chromatin samples had DNA size distributions above dimer size (406 bp) [Figure 2(A)]. The ion-exchange chromatographic technique of Libertini and Small (1980) used to remove histone H1 resulted in a slight selection against the very high molecular weight material in our samples. This can be seen in the appearance of the monomer band in Figure 2(A) for the H1-stripped material. Despite this, more than 98% of H1-stripped chromatin was dinucleosome and greater in size.

Possible nucleosomal sliding due to H1 stripping was monitored by redigesting whole and H1-stripped preparations with increasing concentrations of micrococcal nuclease [Figure 2(B)–(D)]. The multimer peaks are coincident for both whole and H1-stripped material throughout the series, so there is no gross realignment of nucleosome cores along the fiber as histone H1 is removed. Redigested H1-stripped chromatin initially shows a broader multimeric distribution [Figure 2(B)]. This broader distribution may be due to a simple increase in the amount of DNA susceptible to nuclease attack or a randomizing of the nucleosomal spacing due to the stripping process.

Thermal denaturation of control and acetylated whole chromatin in 5 mM sodium displayed a major inflection centered around 82 °C. The derivative of the hyperchromic shift was resolved in all cases into three reproducible transitions (Figure 3, protein/DNA ratio = 1.3; see Table I): two minor components centered at 68 and 73 °C (transitions I and II) and a major component centered at 81 °C (transition III). Overall, we observed no dependency of T_m values on protein

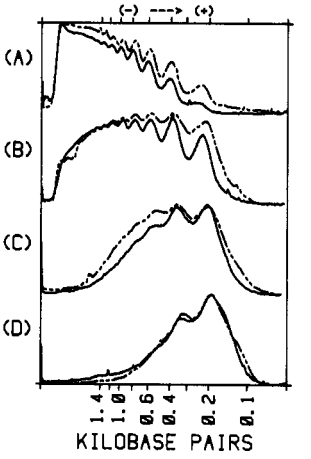

FIGURE 2: Densitometry scans of micrococcal nuclease digests of whole (—) and H1-stripped (- - -) hyperacetylated chromatin. Tracing A is from material as originally prepared. Tracings B–D are from material redigested at increasing nuclease activities. DNA sizes were estimated by using ϕX174/*Hae*III restriction fragment markers.

degradation at 5 mM sodium ion concentration. An important exception was a 4.5 °C decrease in T_m to about 63.5 °C for the premelt region (transition I) upon removal of histone H1 for both hyperacetylated and control chromatin. This is well outside the range of experimental error (Table I). Pure HeLa DNA from these samples melted at 62.9 °C; assuming 40.3% G-C content in HeLa chromatin (Guttman et al., 1977), the theoretical melting point should be 61.0 °C at these ionic strengths (Wada et al., 1980). Thus, the premelt region evidently melts as protein-free DNA after removal of H1 histone.

Thermal melting studies at 0.2 mM EDTA show very few differences between control and hyperacetylated chromatin, especially preparations without H1 histone (Table I). As with Reczek et al. (1982), we see an increase in hyperchromicity

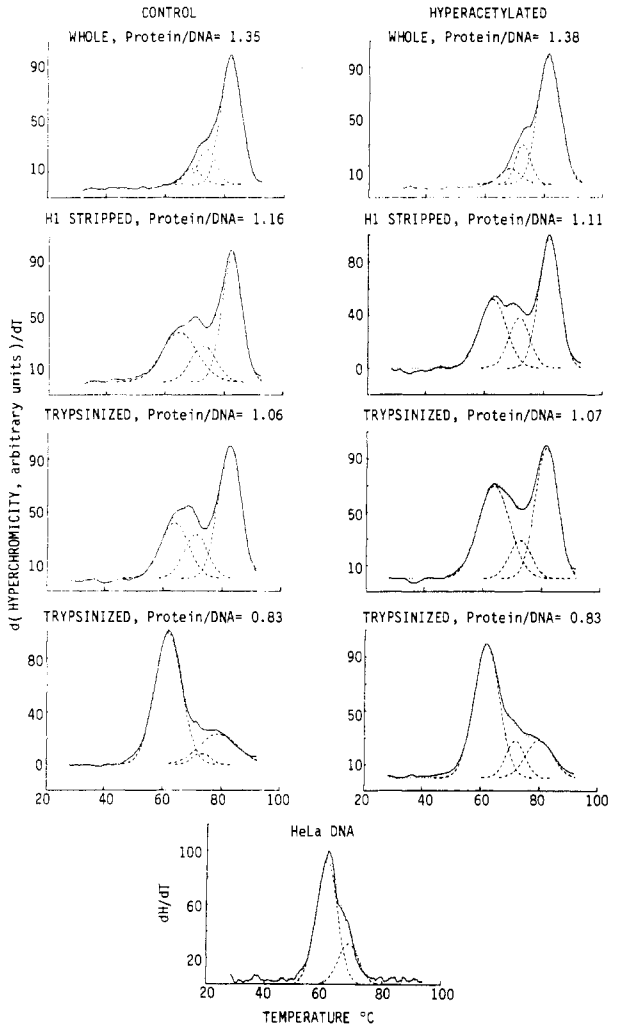

FIGURE 3: Thermal melting profiles of control and hyperacetylated chromatin preparations. Each plot is normalized to maximum amplitude, and the derivative of the hyperchromicity as a function of temperature in the ordinate is in arbitrary units. The type of preparation and its protein/DNA ratio are noted at the top of each plot.

in transition III for acetylated samples with somewhat lower transition melting points when compared to control whole chromatin. These differences seem to disappear when H1 histone is removed as reported previously (Reczek et al., 1982; Huvos et al., 1984; Sasi & Fasman, 1984).

The protein-dependent hyperchromicities of the three major melting transitions differ significantly between control and hyperacetylated chromatin at 5 mM sodium phosphate. This is seen qualitatively in the melting profiles of Figure 3 and is shown more quantitatively in Figure 4 in which percent hyperchromicity is plotted as a function of protein/DNA ratio. In Figure 4, whole and H1-stripped chromatin points are averaged since histone H1 was removed by using ion-exchange chromatography. The intermediate transition II remains approximately constant in area for control chromatin samples upon partial removal of the N-termini of the core histones, H3, H4, H2a, and H2b. This is illustrated in Figure 3 for protein/DNA = 1.06, at which point H3 and H4 N-termini have been partially removed; data for H2a and H2b are not shown. For both control and hyperacetylated chromatin, DNA melting in transitions II and III is shifted in the direction of the premelt transition I as protein is removed (Figure 4). It is seen from comparing slopes in Figure 4 that control samples show a significantly greater dependence on protein content in transitions I and II for the H1-stripped and trypsinized data points. The situation is reversed for hyperacetylated preparations which show a greater dependency on protein content in transition III and only a slight dependence in transition II.

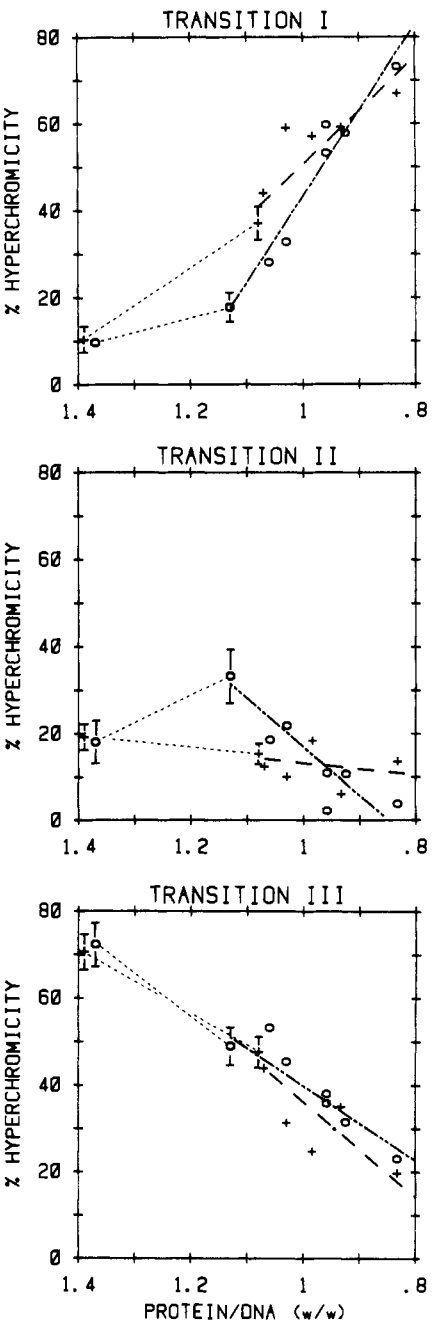

FIGURE 4: Protein-dependent behavior of the percent hyperchromicity for the three resolved melting transitions for control (O−·−O) and hyperacetylated (+−−+) chromatin. The points with error bars (±1 standard deviation) for whole and H1-stripped chromatin at protein/DNA ratios of 1.38 and 1.10, respectively, are average values from seven and four preparations. The protein/DNA axis is inverted left to right, beginning (left) at values for whole chromatin and continuing down to values obtained after maximal trypsinization (right). Linear regression fits to the data shown have confidence limits >99%.

In Figure 4, we use linear regression to represent the trends in the protein-dependent behavior of the percent hyperchromicity. This, in effect, treats the percent hyperchromicity as a continuous function of the degree of trypsinization. It may be argued that such data are really step functions since the core histones are degraded selectivity with trypsin, and large deviations might occur when a particular histone is proteolyzed. A test for the adequacy of the linear approximation is to compare the total hyperchromicity of nontrypsinized samples (protein/DNA ratio of about 1.1) to that

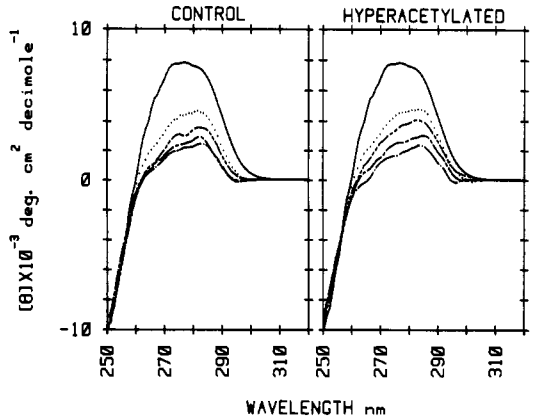

FIGURE 5: Circular dichroism spectra of control and hyperacetylated chromatin preparations: whole chromatin (-•-) with a protein/DNA ratio of 1.45 (control) and 1.44 (hyperacetylated); H1-stripped chromatin (-·-) with a protein/DNA ratio of 1.14 (control) and 1.11 (hyperacetylated); trypsinized chromatin (-···-) with a protein/DNA ratio of 0.959 (control) and 0.984 (hyperacetylated); trypsinized chromatin (···) with a protein/DNA ratio of 0.833 (control and hyperacetylated); purified DNA (—).

obtained as the sum of the linearly extrapolated values for the three resolved transitions at limit trypsin digest conditions (protein/DNA ratio of 0.8). It is clear from Figure 4 that in both cases, the extrapolated percent hyperchromicities for the three transitions sum to roughly 100% for both control and hyperacetylated data.

CD spectra (Figure 5) at 5 mM sodium phosphate of whole chromatin showed an average molar ellipticity of 2650 deg cm^{-2} $dmol^{-1}$ for control and 2460 deg cm^{-2} $dmol^{-1}$ for hyperacetylated material at 282.5 nm. These intensities are suppressed compared to published values (Fulmer & Fasman, 1979; Watanabe & Iso, 1981; Reczek et al., 1982). Pure DNA from HeLa chromatin showed a molar ellipticity of 7388 deg cm^{-2} $dmol^{-1}$ at the same wavelength. This is also somewhat lower than values of 9000 deg cm^{-2} $dmol^{-1}$ reported for DNA from other chromatin preparations (Cowman & Fasman, 1978). We can offer no explanation other than possible differences in sample preparation to account for this apparent suppression in CD intensities, and we attach no significance to it. However, to facilitate comparison to published data, we have adopted the analytic method of MacDermott (1985) where the integrated molar ellipticity of the sample (R_x) is normalized to that of pure DNA (R_0). This helps to minimize possible systematic errors of measurement. The ratios R_x/R_0 of integrated molar ellipticities between 260 and 300 nm for chromatin to protein-free DNA were identical within experimental error (Figure 6), and both reached a maximum of about 53%.

Discussion

In this work, we have combined CD spectra in a novel way with TD to provide additional information on the local conformational behavior of the three principal regions of stability in the nucleosome. Using data published by Cowman and Fasman (1978, 1980), we observe a high level of correlation between the fractional or normalized integrated CD spectral intensity for the band above 260 nm, R_x/R_0, and the length of DNA for mononucleosomes containing DNA in excess of 146 bp (Figure 7). A similar correlation is found for particles both containing and stripped of histones H1 and H5. It is seen from Figure 7 that linear regressions on both systems have the same slope, but the intercept is larger for the H1/H5-stripped particles. This increase may be due to the contribution of an additional 30–40 bp of unfolded DNA to the CD spectral

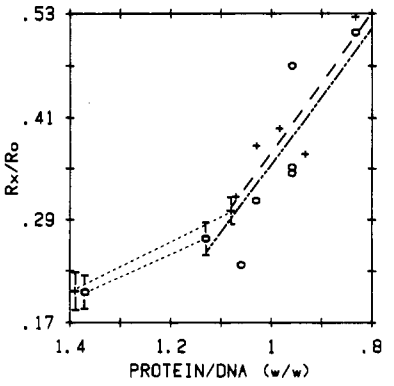

FIGURE 6: Protein-dependent behavior of the normalized integrated band intensity of control (O-··-O) and hyperacetylated (+--+) chromatin. The points with error bars (±1 standard deviation) for whole and H1-stripped preparations are averages of seven and four different preparations, respectively (see Figure 4). The line shown for data from H1-stripped and trypsinized preparations is a linear regression with confidence limit >99%.

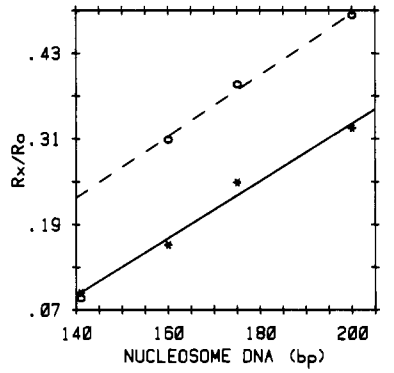

FIGURE 7: Linker DNA-dependent increase in the normalized CD integrated spectral intensities of unperturbed (containing H1/H5 histones) (★—★) and perturbed (stripped of H1 and H5) (O---O) mononucleosome preparations containing various lengths of DNA. Data are from Cowman and Fasman (1978, 1980). The integrated intensity of the positive band above 259 nm was normalized by the integrated intensity of the same band for DNA isolated from the preparations. Each point is an average of two to seven preparations. The correlation coefficient for the linear regression is 0.984.

intensity. This type of unfolding has been shown to occur in core particles at low salts, is inhibited by histone H1, and is promoted by core DNA lengths in excess of 160 bp (Burch & Martinson, 1980). We conclude, therefore, that there is a direct, linear relationship between the amount of relaxed B-form DNA in nucleosomes and the integrated CD spectral intensity for the band above 260 nm.

The relationship between R_x/R_0 and relatively unstressed or "linker-like" DNA can be used with appropriate caution to assist in assigning observed TD transitions to the principal regions of DNA in chromatin: linker, flanking, and central loop DNA. Since the TD and CD were parallel measurements, it is appropriate to compare them directly. This procedure is independent of protein/DNA ratio analysis, and errors in this quantity have no effect upon the conclusions drawn.

The following arguments are based upon a comparison of data in Figures 4 and 6. It is clear that a *positive* correlation exists between percent hyperchromicity of transition I and R_x/R_0 for both control and hyperacetylated samples. Linear regression analyses for both samples are identical within experimental error and account for over 91% of the variation of the samples (control r = 0.9111, hyperacetylated r = 0.9124). This suggests assignment of this premelt transition to the linker DNA region, consistent with a similar assignment in nucleosomes by others (Reczek et al., 1982; Cowman &

Fasman, 1980). The same analysis for transition II shows very little correlation and accounts for less than half of the variation of the sample (control $r = 0.2334$; hyperacetylated $r = 0.4541$). This emphasizes the importance of protein/DNA ratios in describing the changes in content of the intermediate transition, which we assign to the flanking region of the nucleosome.

There is a *negative* correlation between the amount of material melting in transition III and R_x/R_0, characteristic of a fixed size, relatively highly stressed central core region. This assignment is consistent with that of Weischet et al. (1978). In transition III, control and hyperacetylated samples fall on different regression lines, and although the intercepts are the same, the slope for hyperacetylated samples, −213 ($r = -0.8788$) in normalized units, is significantly greater than the slope of the control which is −163 ($r = -0.8813$). This suggests significant, if not direct, interaction between histone hyperacetylated regions and the central core DNA. All of the above seems to imply that the central core is the major source of the additional unstressed DNA melting in transition I as the core histones are trypsinized, with the destabilization process evidently more efficient in hyperacetylated chromatin.

Table I lists percent hyperchromicity data calculated as the amount of DNA in base pairs melting in each of the three resolved transitions on the basis of a nucleosomal repeat of 203 bp. In interpreting these results, it is useful to distinguish four principal regions of stability in the nucleosome [terminology from Yau et al. (1982)]: (1) central core DNA which melts cooperatively in transition III; (2) flanking DNA which with the central core DNA makes up the nuclease-resistant 146 bp core particle; (3) loose core DNA which completes the 168 bp chromatosome; (4) linker DNA which is in excess of chromatosomal DNA.

In whole chromatin, the central core accounts for 143–146 bp of DNA. Histone H1 evidently interacts with DNA in the linker region, stabilizing about 20 bp and causing it to melt with loose core DNA in transition II. Removal of H1 seems to destabilize the entire nucleosome, with core DNA now accounting for only a little more than one superhelical turn of 96–99 bp, leaving flanking DNA to melt separately in transition II. The two highest melting transitions in H1-stripped control chromatin account for 166 bp of DNA, and the flanking DNA appears to melt in transition II with loose core DNA. In H1-stripped hyperacetylated chromatin, the two highest melting transitions account for only 127 bp, so the loose core DNA appears to melt with linker DNA in transition I. Thus, destabilizing the loose core DNA may be one effect of histone acetylation.

Below 1.5 mM sodium, core particles evidently unfold, and a similar effect is observed when core histone tails are removed. It is possible, therefore, that differential stability effects due to hyperacetylation of the N-terminal histone domains may be obscured at ionic strengths at or below the nucleosomal low-salt transition. Results from the present study shown in Table I and elsewhere are consistent with this interpretation.

In Figure 4, control chromatin appears to maintain a strong protein/DNA dependence for DNA melting in the flanking (transition II) and linker (transition I) regions as the core histones are trypsinized. Hyperacetylated chromatin, however, shows little protein–DNA dependence in the flanking region but an increased dependence for central core DNA (transition III). These results suggest that acetylation decreases protein–DNA interactions in the flanking region. At the same time, central core DNA in acetylated chromatin appears more sensitive to loss of core histone tails than in the nonacetylated control.

In using the procedure of Fraser and Suzuki (1966), we have made two assumptions which appear justified in view of previous studies. First, we assume that all melting profiles can be resolved into a sum of three Gaussians and, second, that T_m is a satisfactory criterion for consistent resolution along the series of whole, H1-stripped, and trypsinized chromatin samples. The first assumption is supported by a variety of other studies (Van Holde et al., 1980; Cowman & Fasman, 1980; Reczek et al., 1982; Yau et al., 1982, 1983). Resolution beyond three Gaussians is normally not justified on mathematical grounds, but the technique may be capable of higher levels of quantitation than we have been able to achieve to date (Kaplan et al., 1984; Yau et al., 1982). The reason we see no reproducible differences in T_m for control and hyperacetylated chromatin seems to derive from the use of T_m as a criterion for consistent resolution. We determined this relationship for the T_m after initially studying the correlation between the CD integrated spectral intensity and percent hyperchromicity from TD experiments.

Our semiquantitative interpretation of CD results is justified by standard chiroptic theory for polymers in terms of specific conformational parameters [for a review, see Charney (1979)]. Theoretical studies have shown that the positive exciton band for DNA in chromatin above 260 nm is suppressed due to irregularities in the B-form helix induced by supercoiling (MacDermott, 1985) and that exciton coupling is dependent on base pair tilt and chromophore displacement from the helix axis (Studdert & Davis, 1974; Moore & Wagner, 1973; Baase & Johnson, 1979). The effects of tertiary interactions (Cowman & Fasman, 1978) between bases of different supercoils appear to cancel. However, the relationship between chiral activity and superhelical density is complex, and data are not available to allow a higher level of quantitation than we have utilized here. Furthermore, protein–DNA interactions appear to be irregular and somewhat localized (Richmond et al., 1984; Frederick et al., 1984), and the effect of tightly bent regions in the DNA helix is presently unknown.

CD spectra are nevertheless highly sensitive to conformation on an overall or *global* basis. It is evident from the behavior of R_x/R_0 shown in Figure 6 that in vivo hyperacetylation has a negligible effect upon the global structure of chromatin. These data suggest that *global* conformational changes for DNA in chromatin induced by trypsinolysis of the core histones are not affected by the levels of acetylation reported here. Thus, DNA stability changes reported in this and in prior studies must occur locally and in such a manner as to be effectively self-compensatory with respect to overall DNA conformation. The differential effects in protein-dependent TD which we observe between control and hyperacetylated chromatin therefore imply that hyperacetylation results in an overall loosening of nucleosomal DNA with some loss of both short-range and longer range interfiber interactions but with little or no global changes in chromatin conformation. We speculate, therefore, that a functional role of hyperacetylation in transcriptional chromatin may be to reduce unfolding cooperativity and hence allow a higher level of local control of the unfolding process during transcription.

Conclusions

(1) We observe a direct, positive, linear correlation between the amount of relaxed B-form DNA in the internucleosomal linker region of chromatin and the integrated intensity of the CD spectral band above 260 nm.

(2) Correlated use of CD spectra using the above relationship suggests the following assignments to the three resolved TD transitions in chromatin at 5.25 mM salt: transition

III, the highest melting transition, is highly stressed, central core DNA; transition II, the intermediate transition, is less stressed flanking DNA; and transition I, the lowest melting transition, is relatively unstressed loose core/linker DNA.

(3) Using the above assignments, we have resolved observed TD transitions for our series of chromatin preparations into sums of three Gaussians and, on the basis of these results, suggest that T_m is an adequate criterion for consistent resolution of these transitions.

(4) In vivo hyperacetylation has a negligible effect upon the *global* conformation of chromatin at 5.25 mM salt as evidenced by CD spectral data.

(5) Control chromatin and hyperacetylated chromatin differ in subtle but significant ways in the thermal stability of DNA in different nucleosomal regions. Hyperacetylation evidently reduces protein–DNA interactions in the loose core DNA of the flanking region.

(6) These differences are reflected also in the dependency of these regions on enzymatic degradation of the core histone unstructured "tails".

(7) Since in vivo hyperacetylation appears to result in an overall loosening of DNA with no evident changes in the overall chromatin structure, we speculate that a functional role of hyperacetylation may be to reduce cooperativity in the unfolding transition during transcription.

References

Allan, J., Harborne, N., Rau, D. C., & Gould, H. (1982) *J. Cell Biol. 93*, 285–297.

Ausio, J., & Van Holde, K. E. (1986) *Biochemistry 25*, 1421–1428.

Baase, W. A., & Johnson, W. C., Jr. (1979) *Nucleic Acids Res. 6*, 797–814.

Bohm, L., & Crane-Robinson, C. (1984) *Biosci. Rep. 4*, 365–386.

Burch, J. B. E., & Martinson, H. G. (1980) *Nucleic Acids Res. 8*, 4969–4987.

Burkhart, R. D., & Howells, P. N. (1979) *J. Chem. Educ. 56*, 249.

Charney, E. (1979) *The Molecular Basis of Optical Activity*, Wiley, New York.

Christensen, M. E., Rattner, J. B., & Dixon, G. H. (1984) *Nucleic Acids Res. 12*, 4575–4592.

Cowman, M. K., & Fasman, G. D. (1978) *Proc. Natl. Acad. Sci. U.S.A. 75*, 4759–4763.

Cowman, M. K., & Fasman, G. D. (1980) *Biochemistry 19*, 532–541.

Crane-Robinson, C., & Bohm, L. (1985) *Biochem. Soc. Trans. 13*, 303–306.

Dimitrov, S., Makarov, V., Apostolova, T., & Pashev, I. (1986) *FEBS Lett. 197*, 217–220.

Fraser, R. D. B., & Suzuki, E. (1966) *Anal. Chem. 38*, 1770–1773.

Frederick, C. A., Grable, J., Melia, M., Samudzi, C., Jen-Jacobson, L., Wang, B.-C., Greene, P., Boyer, H. W., & Rosenberg, J. M. (1984) *Nature (London) 309*, 327–331.

Fulmer, A. W., & Fasman, G. D. (1979) *Biopolymers 18*, 2875–2891.

Grigoryev, S. A., & Krasheninnikov, I. A. (1982) *Eur. J. Biochem. 129*, 119–125.

Guttman, T., Vitek, A., & Pivec, L. (1977) *Nucleic Acids Res. 4*, 285–297.

Hall, J. M., & Cole, R. D. (1985) *Biochemistry 24*, 7765–7771.

Hardison, R., & Chalkley, R. (1978) *Methods Cell Biol. 17*, 235–251.

Harrington, R. E. (1981) *Biopolymers 20*, 719–752.

Harrington, R. E. (1982) *Biochemistry 21*, 1177–1186.

Hjelm, R. P., & Huang, R. C. C. (1974) *Biochemistry 13*, 5275–5283.

Huvos, P., Sasi, R., & Fasman, G. D. (1984) *Biopolymers 23*, 2195–2210.

Kaplan, L. J., Bauer, R., Morrison, E., Langan, T. A., & Fasman, G. D. (1984) *J. Biol. Chem. 259*, 8777–8785.

Laemmli, U. K. (1970) *Nature (London) 227*, 680–685.

Libertini, L. J., & Small, E. W. (1980) *Nucleic Acids Res. 8*, 3517–3534.

Lilley, D. M. J., & Tatchell, K. (1977) *Nucleic Acids Res. 4*, 2039–2055.

Lowry, O. H., Rosebrough, N. J., Farr, A. L., & Randall, R. J. (1951) *J. Biol. Chem. 193*, 265–275.

MacDermott, A. J. (1985) *Philos. Trans. R. Soc. London, A 313*, 453–505.

Marion, C., Roux, B., Pallotta, L., & Coulet, P. R. (1983) *Biochem. Biophys. Res. Commun. 114*, 1169–1175.

Matthews, H. R., & Waterborg, J. H. (1985) in *The Enzymology of Post-translational Modification of Proteins* (Freedman, R., & Hawkins, H. C., Eds.) Vol. 2, pp 125–185, Academic Press, London.

McGhee, J. D., Nickol, J. M., Felsenfeld, G., & Rau, D. C. (1983) *Nucleic Acids Res. 11*, 4065–4075.

Moore, D. S., & Wagner, T. E. (1973) *Biopolymers 12*, 201–221.

Noll, M., Thomas, J. O., & Kornberg, R. D. (1975) *Science (Washington, D.C.) 187*, 1203–1206.

Reczek, P. R., Weissman, D., Huvos, P. E., & Fasman, G. D. (1982) *Biochemistry 21*, 993–1002.

Richmond, T. J., Finch, J. T., Rushton, B., Rhodes, D., & Klug, A. (1984) *Nature (London) 311*, 532–537.

Riggs, M. G., Whittaker, R. G., Neumann, J. R., & Ingram, V. M. (1977) *Nature (London) 268*, 462–464.

Russev, G., Vassilev, L., & Tsanov, R. (1980) *Mol. Biol. Rep. 6*, 45–49.

Sasi, R., & Fasman, G. D. (1984) *Biochim. Biophys. Acta 782*, 55–66.

Sealy, L., & Chalkley, R. (1978) *Cell (Cambridge, Mass.) 14*, 115–121.

Simpson, R. T. (1978) *Cell (Cambridge, Mass.) 13*, 691–699.

Smith, P. J. (1986) *Carcinogenesis (London) 7*, 423–429.

Studdert, D. S., & Davis, R. C. (1974) *Biopolymers 13*, 1391–1403.

Thomas, J. O., & Kornberg, R. D. (1975) *Proc. Natl. Acad. Sci. U.S.A. 72*, 2626–2630.

Uberbacher, E. C., Ramakrishnan, V., Olins, D. E., & Bunick, G. J. (1983) *Biochemistry 22*, 4916–4923.

Van Holde, K. E., Allen, J. R., Tatchell, K., Weischet, W. O., & Lohr, D. (1980) *Biophys. J. 10*, 271–282.

Wada, A., Yabuki, S., & Husimi, Y. (1980) CRC *Crit. Rev. Biochem. 9*, 87–144.

Watanabe, K., & Iso, K. (1981) *J. Mol. Biol. 151*, 143–163.

Waterborg, J. H., & Harrington, R. E. (1986) *Comput. Methods Programs Biomed. 23*, 255–260.

Waterborg, J. H., Pitter, R., & Harrington, R. E. (1987) *Access, J. Microcomput. Appl.* (in press).

Weintraub, H., & Van Lente, F. (1974) *Proc. Natl. Acad. Sci. U.S.A. 71*, 4249–4253.

Weischet, W. O., Tatchell, K., Van Holde, K. E., & Klump, H. (1978) *Nucleic Acids Res. 5*, 139–160.

Whitlock, J. P., Jr., & Simpson, R. T. (1977) *J. Biol. Chem. 252*, 6516–6520.
Whitlock, J. P., Jr., & Stein, A. (1978) *J. Biol. Chem. 253*, 3857–3861.
Wilhelm, M. L., & Wilhelm, F. X. (1980) *Biochemistry 19*, 4327–4331.
Wu, H.-M., Dattagupta, N., Hogan, M., & Crothers, D. M. (1979) *Biochemistry 18*, 3960–3965.
Yau, P., Thorne, A. W., Imai, B. S., Matthews, H. R., & Bradbury, E. M. (1982) *Eur. J. Biochem. 129*, 281–288.
Yau, P., Imai, B. S., Thorne, A. W., Goodwin, G. H., & Bradbury, E. M. (1983) *Nucleic Acids Res. 11*, 2651–2664.

Comparison of S100b Protein with Calmodulin: Interactions with Melittin and Microtubule-Associated τ Proteins and Inhibition of Phosphorylation of τ Proteins by Protein Kinase C[†]

Jacques Baudier, Daria Mochly-Rosen, Alexandra Newton, Sun-Hee Lee, Daniel E. Koshland, Jr., and R. David Cole*

Department of Biochemistry, University of California, Berkeley, California 94720

Received July 2, 1986; Revised Manuscript Received December 19, 1986

ABSTRACT: To gauge similarities between S100b protein and calmodulin, interactions were observed between S100b and melittin and between S100b and τ, the microtubule-associated proteins. The interaction of melittin with S100b protein in the presence and absence of calcium was studied by fluorescence polarization, UV difference spectroscopy, and sulfhydryl derivatization. Whether calcium was present or not in the solution, melittin and S100b form a complex of molar ratios up to 2:1. Further binding of melittin occurred, but it resulted in precipitation of S100b, as is true of the corresponding case of melittin binding to calmodulin. In the absence of calcium, the interaction of melittin and S100b shielded the tryptophan (Trp) of the former protein and exposed cysteine-84β (Cys-84β) of the latter protein, leaving the tyrosine-16β (Tyr-16β) of S100b unaffected. Calcium addition to the complex partially restored the exposure of Trp of melittin and caused changes in the environment of Tyr-16β (unlike the environmental changes induced for Tyr-16β by calcium in the absence of melittin). The conformational changes induced in S100b by interaction with melittin increased its affinity for calcium and offset the inhibition of calcium binding otherwise observed in the presence of potassium ions. This corroborated the previous finding that S100b affinity for calcium greatly depends on the protein conformation. The phenomena described above are similar to the interactions of melittin with calmodulin and thus suggest that S100b and calmodulin have a common structural domain not only that binds melittin but also that may interact with common target proteins. In support of this suggestion is our observation that S100b, as previously reported for calmodulin, binds to the microtubule-associated protein τ in the presence of calcium, a fact that could explain their common calcium-dependent effects on microtubule assembly. Complex formation of τ with S100b or calmodulin was confirmed when we discovered that both S100b and calmodulin inhibit the calcium/phospholipid-dependent phosphorylation of τ proteins by protein kinase C by interacting with the substrate rather than with the kinase itself.

S100b is a cytosolic, acidic protein that belongs to the calcium binding protein family of the "EF-hand" type (Isobe & Okuyama, 1978). While present mainly in glial cells of the central nervous system (Ghandour et al., 1981), it has also been found in several nonnervous tissues [for a review, see Molin et al. (1984)]. The biological function of S100b protein remains unproven, but it is clear that S100 proteins affect the in vitro assembly and disassembly of microtubules (Baudier et al., 1982; Donato, 1983; Endo & Hidaka, 1983), modulate the phosphorylation of a 19-kilodalton (19-kDa)[1] brain protein by protein kinase X (Qi & Kuo, 1984a,b), and inhibit the phosphorylation of a soluble 73-kDa brain protein (Patel et al., 1983).

Although S100 protein and calmodulin are clearly different proteins and have different distributions in the brain (Tabuchi et al., 1984), they are structurally related and share some physicochemical properties. They both bind to phenothiazine–Sepharose columns (Marshak et al., 1981) and to melittin–Sepharose columns (Kincaid & Coulson, 1985) in a calcium-dependent manner. Furthermore, the majority of brain proteins, including calcineurin, that bind to S100–Sepharose also bind to calmodulin–Sepharose and vice versa (Gopalakrishna et al., 1985), suggesting that both of the latter proteins might regulate some target proteins in common. For instance, a Ca^{2+}-dependent function mediated by calmodulin,

[†] This work was supported by grants from the Institut National de la Santé et de la Recherche Medicale, Centre National de la Recherche Scientifique, by U.S. Public Health Service Grants EHS-ES-01896 and GMS-20338, and by the Agricultural Research Station. Support for J.B. was from a NATO Fellowship and a USPHS International Research Fellowship.

[1] Abbreviations; Trp, tryptophan; Tyr, tyrosine; Cys, cysteine; FPLC, fast-protein liquid chromatography; DTNB, 5,5′-dithiobis(2-nitrobenzoic acid); DTE, dithioerythritol; SDS, sodium dodecyl sulfate; EGTA, [ethylenebis(oxyethylenenitrilo)]tetraacetic acid; kDa, kilodalton(s); EDTA, ethylenediaminetetraacetic acid; Tris, tris(hydroxymethyl)-aminomethane.

0006-2960/87/0426-2886$01.50/0